Lowpass and Bandpass Filter Designs Based on DGS with Complementary Split Ring Resonators

Ghofran E. Al-Omair, Samir F. Mahmoud, and Ayman S. Al-Zayed

Electrical Engineering Department
Kuwait University, P.O. Box 5969, Al-Safat, 13060, Kuwait
alomair_g@hotmail.com, samir.hadi@ku.edu.kw, ayman.alzayed@ku.edu.kw

Abstract ─ We present novel designs of compact lowpass filters (LPF) and bandpass filters (BPF) based on defected ground structures (DGS) using two complementary split ring resonators (CSRR) that are etched in the ground plane. The geometries of the two CSRRs, of unequal areas, are optimized for a LPF with sharp cutoff and wide stop band. For the design of the BPF, a gap capacitor is added in series with the main transmission line and the two or three etched CSRRs are designed to achieve a given bandwidth, and a wide rejection band. Simulation results on the SEMCAD-X software are compared with circuit models and measurements on fabricated lowpass and bandpass filters.

Index Terms ─ Defected ground structures, microstrip circuit, microwave filters.

I. INTRODUCTION

Modern wireless communication systems call for compact size, low cost, and high performance components. Microwave filters are essential components in such systems and much effort has been spent recently to design compact lowpass and bandpass filters with sharp cutoff and wide stop band performance. One technique to shape filter response is to include photonic band gap (PBG) structures in filter design. This is done by etching a set of periodic defects in the ground plane of a microstrip structure. These PBG structures have the character of producing band gaps or stop bands that shape the filter response [1-3]. In addition to their stop band behavior, they have the property of slowing down the propagating electromagnetic waves, which tends to reduce the filter dimensions. However, in order to show their band gap effect, the PBG structures require the presence of many periodic cells [4, 5], which ousts the design compactness. Recently, new DGS shapes have been proposed by several authors as means of filter design by using only one or few cells. Commonly used DGS shapes include the dumbbell shape [5], the H-shape [6], the interdigital slot [7] and the split ring resonator [8-14].

A cell of such DGS disturbs the shield current in the ground plane and can increase the inductance and capacitance of the strip line. A single dumbbell defect has been modeled as a parallel L-C circuit connected in series with the line [5] and therefore acts as a one-pole lowpass filter. A similar model has been adopted for the H defect and other defects [15]. The slow wave factor caused by one or more DGS has been studied in [16].

A LPF with wide stop band has been designed on a ground plane with two dumbbell defects in [5] and with three dumbbell defects in [4]. A bandpass filter based on three sections of coupled lines on a three dumbbell defected ground has been presented in [17]. The DGSs enhance the coupling between coupled lines, which increases the filter bandwidth from 14% with no DGSs to 42%.

The use of H-shaped defect is found to result in a more compact LPF compared to one using dumbbell defects [6, 15, 18]. A crescent shape DGS structure has been utilized to design a lowpass filter [19]. A microstrip bandpass filter has been designed based on folded tri-section step impedance resonator and slotted ground defects [20].

The split ring resonator (SRR) is a building block in periodic structures behaving as metamaterial with negative permeability around its resonant frequency [11, 12]. The complimentary split ring resonator (CSRR) has been utilized as a DGS for filter design [13, 14]. The CSRR has

Submitted On: April 4, 2011
Accepted On: Oct. 28, 2011

been modeled as a parallel L-C circuit connected between the line capacitor and the ground [8, 10]. A LPF with sharp rejection has been designed based on the use of 3 CSRRs in [21]. The filter stop band has been increased by properly orienting the CSRR relative to the printed line [22]. A bandpass filter based on a pair of coupled lines and three CSRRs DGS is presented in [23]. The CSRRs tend to increase the coupling between the lines and increase the filter bandwidth. A bandwidth of 1 GHz about a center frequency of 3.5 GHz has been reported [23].

In this paper, we present a simple design of compact LPF using two or three CSRR DGS. The microstrip transmission line joining the input to the output is a uniform 50Ω line with no discontinuities or connected stubs. The distances between the defects and their areas are optimized to obtain a filter with sharp cutoff and wide stop band. In addition, a bandpass filter is designed by using two or three CSRRs and a gap capacitor connected in series with the main printed line.

The proposed LPF is introduced in the next section along with an equivalent circuit model. The latter is compared with simulation results taken on SEMCAD-X software. Similarly, the proposed BPF is presented in Section III along with its circuit model and simulation results. The capability of enhancing the rejection band is illustrated in this section by adding a third CSRR defect. Several versions of the LPF and BPF are built and tested. Measurements on both filters are compared with simulations in Section IV. The conclusions are drawn in Section V.

II. DESIGN AND GEOMETRY OF THE LOWPASS FILTER

The geometry of the proposed LPF is shown in Fig. 1a, where a 50 Ω strip line is printed on the dielectric layer surface and two CSRRs are etched in the ground plane. The two complementary SRRs are similar to one another except that the smaller ring (A2) is rotated by 90° relative to the larger ring (A1). The area of both rings and the spacing between them are design parameters that must be properly chosen in order to obtain a favorable filter response. The CSRR main parameters are shown in the inset of Fig. 1a. These are the slot width (t), the slot gap (g), the spacing (c) between inner and outer rings, and the side length (a). The role of these parameters in shaping the LPF response has been studied in [8, 16]. The circuit model of the LPF is shown in Fig. 1b, where each ring is modeled by a parallel L-C circuit (L3, C3 and L4, C4) connected in series with the line capacitance [8]. The distance between the centers of the CSRRs is modeled by a transmission line (TL) of a given electrical length (θ) at the cutoff frequency.

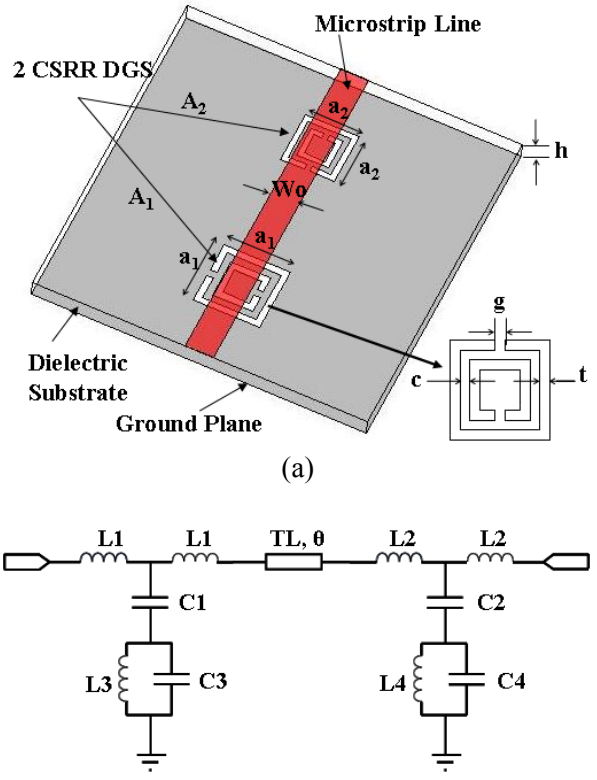

Fig. 1. (a) Geometry of the proposed lowpass filter. (b) Equivalent circuit model.

Using the simulation tool SEMCAD X, we have designed a LPF with the response shown in Fig. 2. The notch frequency of S_{21} at f =2.7 GHz is mainly determined by the dimensions of ring (A1), which is the first (larger) CSRR. The second notch frequency at 3.45 GHz is mainly determined by ring (A2) whose linear dimensions are 85% of ring (A1). The dimensions of ring (A2) influence the stop band, which extends up to 4.75 GHz. The flatness of the pass band response is affected by the dimensions (t), (g), and (c) of the two CSRRs. The simulated S_{11} response lies below -10 dB in the passband. The dimensions of the two CSRRs

used in the LPF of Fig. 2 are tabulated in Table 1 along with the spacing (D) between the centers of the two rings. It is important to note that the rotation of the smaller CSRR by 90° relative to the first one has a major role in achieving the low response level over the wide stop band of the filter. The total length of the filter is about 40 mm. This amounts to one third of the free space wavelength at the 3-dB cutoff frequency (2.5 GHz).

To obtain the equivalent circuit model of the presented LPF, we optimize the circuit elements of Fig. 1b on the Agilent's advanced design system (ADS) software so as to match the simulated S_{21} response. The inferred circuit model S_{21} response is compared with the simulated one in Fig. 2. A good match is observed, particularly in the pass band region. The corresponding values of the circuit elements are tabulated in Table 2. In particular, we note that the electrical length between the centers of the two CSRRs is 140 degrees at 2 GHz. This is certainly influenced by the slow wave effect caused by the CSRR defects [10]. Namely, the effective relative permittivity is about 4.66 in the presence of the defects. Finally, we note that as (A2) is reduced in area while (A1) is kept fixed, the stop band extends to higher frequencies, but the response can exceed the -10 dB limit. A good design ratio of a2/a1 is found to lie between 0.75 and 0.85.

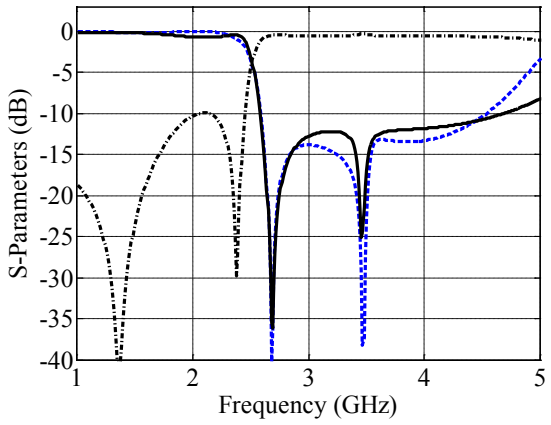

Fig. 2. Comparison between simulated S_{21} (solid line) and circuit model (dashed line) results of the proposed lowpass filter. The simulated S_{11} is shown as dash-dot line. The substrate used has thickness h=1.5 mm and dielectric constant of 2.55.

Table 1: Geometric design parameter details of the proposed lowpass filter in millimeter

a1	t1	s1	c1		
10	1	1	1		
a2	t2	s2	c2	W_o	D
8.5	0.85	0.85	0.85	4.19	27

Table 2: Extracted equivalent circuit parameters of the proposed lowpass filter (Capacitors in (pF), Inductors in (nH))

C1	L1	C2	L2	
0.912	2.5	1.02	2.16	
C3	L3	C4	L4	θ
1.26	1.62	1.136	0.973	140°

It is worth comparing our lowpass filter response with that introduced in [8]. While the two filter responses are comparable to each other our proposed filter does not require any open stubs loading the conductor line.

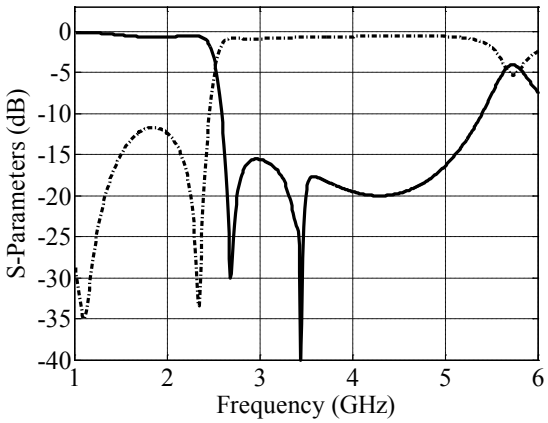

Fig. 3. Simulation results of S_{21} and S_{11} of the three CSRRs LPF. The third ring is 97% of the second ring and is spaced by 20 mm from the second ring.

In order to extend the stop band to higher frequencies, a third CSRR is etched down the line. The added ring size and distance from the second ring are optimized for extended stop band. The simulated result for S_{21} and S_{11} is shown in Fig. 3. The S_{21} is maintained below -15.5 dB in the stop band that extends to 5.1 GHz. This is a definite improvement to the two-CSRR design. The total length of the filter has been increased by 55% compared with the filter using two CSRR defects. It is instructive to compare our three-CSRR with that given in [21] in which the same number of

CSRR's is used. The frequency responses are comparable except that the transition to the stop band is sharper in our design In addition; the strip line in our design is uniform in contrast with the non-uniform line in [21].

III. DESIGN AND GEOMETRY OF THE BANDPASS FILTER

The geometry of the proposed bandpass filter (BPF) is shown in Fig. 4a, where a 50 Ohm line is printed on the dielectric layer and two CSRRs are etched in the metallic ground plane. The line has a series capacitance in the form of an L-shaped gap as shown in the inset of the figure. The two CSRRs are similar in shape and orientation, but have different areas; the second one down the line being the smaller ring ($b_2/b_1<1$). The design parameters shown in Fig. 4a can be carefully adjusted to obtain the desired bandpass filter response.

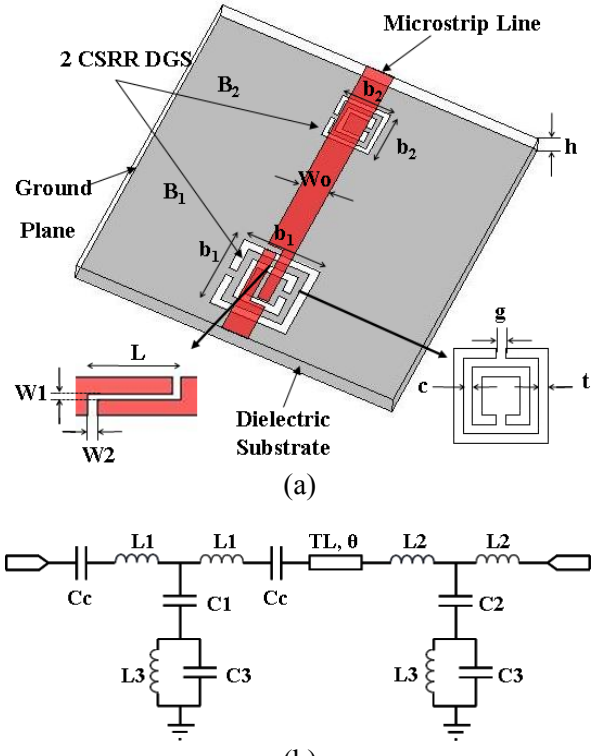

Fig. 4. (a) Geometry of the proposed bandpass filter. (b) Equivalent circuit model.

The design parameters given in Table 3 are the result of a series of simulations using SEMCAD-X software to reach the bandpass response shown in Fig. 5. The L like gap and the large CSRR (B1) influence the low frequency notch at 1.8 GHz, and the attenuation level of the lower band. The smaller CSRR (B2) determines the second notch at 3.7 GHz. It should be pointed out that the two CSRRs must have the same orientation in order to obtain a flat bandpass response. The EM simulated S_{11} is well below -10 dB in the passband. The total filter length is about 45 mm, which amounts to 0.41 of the free wavelength at the midband frequency (2.75 GHz).

An equivalent circuit model of the proposed bandpass filter is shown in Fig. 4b. It clearly resembles that of the LPF (in Fig.1b) except for the added series capacitor (Cc) that represents the L cut. The values of the equivalent inductors, capacitors, as well as the transmission line length between the centers of the two rings were optimized so as to match the simulated S_{21} filter response by using the ADS software. The optimized circuit parameters are summarized in Table 4. The response of the simulated and modeled bandpass filter show good agreement of S_{21} as observed in Fig. 5.

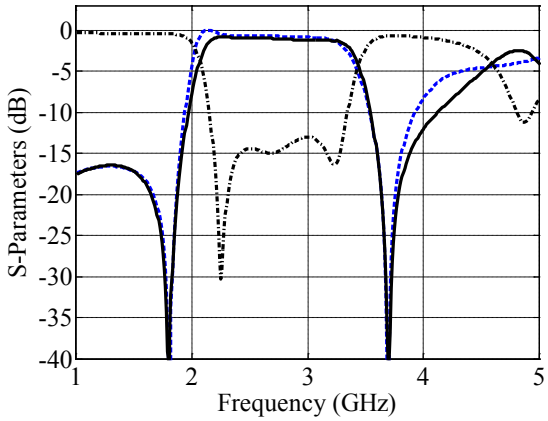

Fig. 5. Comparison between simulation (solid line) and circuit model (dashed line) results for S_{21} of the proposed bandpass filter. The simulated S_{11} is shown by the dash-dotted line. The substrate used has thickness h=1.5 mm and dielectric constant of 2.55.

In an attempt to extend the stop band to higher frequencies, we have added a third CSRR defect down the line. The added CSRR has smaller dimensions and is rotated by 90° relative to the other two rings. This result is an extension of the stop band up to 5.52 GHz compared to 4.5 GHz for the case of two rings; the attenuation level was also improved as shown in Fig. 6.

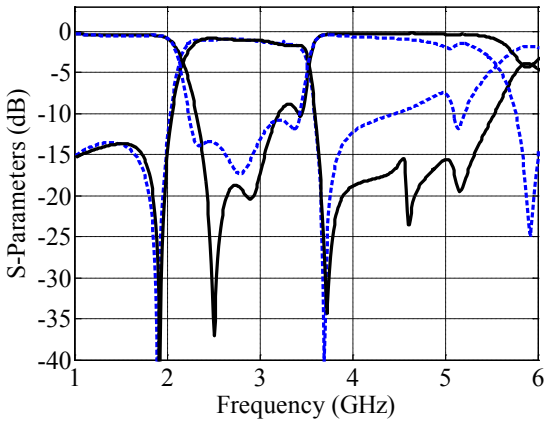

Fig. 6. Simulation results of S_{21} and S_{11} of the three CSRRs BPF with wide stop band (solid lines) compared to the two CSRRs BPF (dotted lines). The third ring is 86.67% of the second ring and is spaced by 21 mm from the second ring.

Table 3: Geometric design parameter details of the proposed bandpass filter in millimeter

b1	t1	s1	c1	b2	t2	s2
12	1.2	1.2	1.2	7.5	0.75	0.75

c2	W_o	D	L	W1	W2
0.75	4.19	31	10	0.6	1

Table 4: Extracted equivalent circuit parameters of the proposed bandpass filter (Capacitors in (pF), Inductors in (nH))

C1	L1	C2	L2	C3
1.77	2.86	0.73	1.82	1.44

L3	C4	L4	Cc	θ
2.43	0.91	1.13	0.86	111.6°

IV. FABRICATIONS AND MEASUREMENTS

In order to verify the design method of the proposed filters, several lowpass and bandpass filters were fabricated and tested using a network analyzer. All of the lowpass and bandpass filter designs were implemented on Taconix/TLX-8 substrate with dielectric constant εr =2.55, height h=1.5 mm, and loss tangent = 0.002. These values are the same as those used for all of the simulations.

Figure 7 shows photographs of the top side (a) and bottom side (b) of the manufactured lowpass. The 90 degree rotation of the smaller CSRR can be seen. Two lowpass filters were fabricated and measured. The first one is the implementation of the one given in Fig. 2. The second fabricated lowpass filter has a larger ring (A1) which was scaled up by about 15% (so that a_2 was increased from 10 to 11.5 mm). The electromagnetic simulation and the measured results of these two filters are shown in Fig. 8a and 8b, respectively. A good agreement is observed between the measurements and simulations. We note that the cutoff frequency of the second LPF (Fig. 8b) is lower than that for the one in Fig. 8a. This is a result of the larger dimensions of the (A1) ring.

Figure 9 shows photographs of the top side (a) and bottom side (b) of the fabricated bandpass filter of Fig. 5 with the parameters listed in Table 3. The simulated and measured results for this bandpass filter are presented in Fig. 10a and good agreement is observed. The measured 3dB bandwidth of the first filter is 1.38 GHz, while the best insertion loss is 0.86 dB measured at 2.06 GHz.

Another BPF with scaled down second ring (B2) by 6.7% (b_2 is reduced 7 mm) is built and measured. The simulation and measurement results of this filter are shown in Fig. 10b. Notice that the second notch frequency is shifted to a higher frequency relative to that in Fig. 10a as one would expect. The measured 3dB bandwidth of this filter is 1.6 GHz, while the best insertion loss is 0.82 dB measured at 2.25 GHz.

V. CONCLUSION

We have presented novel and simple designs of compact LPF and BPF based on DGS using two or three CSRRs of different areas. The desired filter responses are achieved by using a simple 50 ohms transmission line, without the need for step impedances or any junction discontinuity which yield design simplicity. The performance of these filters has been verified by simulations, circuit models, and measurements on fabricated prototypes. The smaller CSRR in the proposed LPF is rotated by 90° relative to the larger one. This is necessary to obtain an acceptable stop band response. It is demonstrated that the cutoff frequency of the LPF is mainly controlled by the geometry and the area of the larger CSRR, while the second CSRR determines the extent of the stop band. Adding a third ring will extend the stop band

as well as improve the attenuation level in the rejection band.

The proposed BPF contains two CSRR ground defects of different areas but having the same orientation. In addition, a gap capacitor is connected in a series with the main printed line. It is demonstrated that the gap capacitor and the first CSRR defect (B1) control the low frequency response and the first cutoff frequency (fc1) while the second CSRR defect (B2) controls the higher cutoff frequency (fc2), hence the filter bandwidth. It has been demonstrated that a third smaller CSRR defect, added down the line, can significantly improve the upper stop band and extends it to higher frequencies (Fig. 6). The measured filter responses on manufactured LPFs and BPFs have shown excellent agreement with simulated results.

ACKNOWLEDGEMENT

Dr. Ayman Al-Zayed would like to acknowledge Kuwait University for their support and making his sabbatical leave during the academic year 2010-2011 successful.

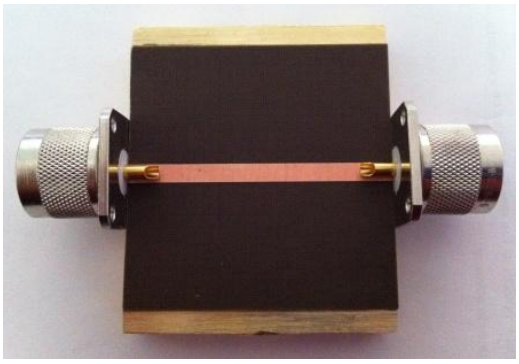

(a)

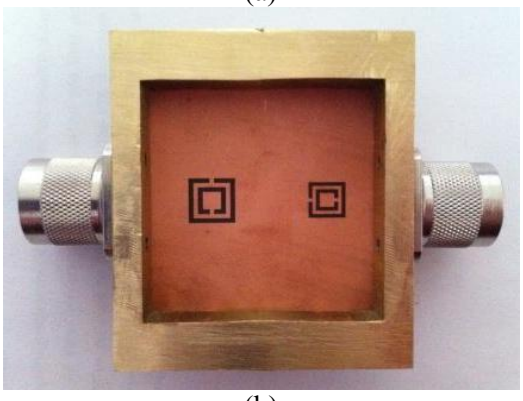

(b)

Fig. 7. Photographs of the fabricated lowpass filter (a) Top side. (b) Bottom side.

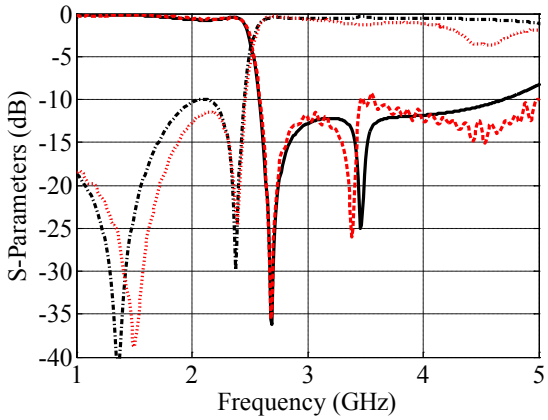

Fig. 8a. Simulation results compared to measured results of the proposed lowpass filter of Fig. 2. Simulated S_{21} and S_{11} are shown as (solid), (dash-dot) lines, respectively. Measured S_{21} and S_{11} are shown as (dashed) and (dotted) lines, respectively.

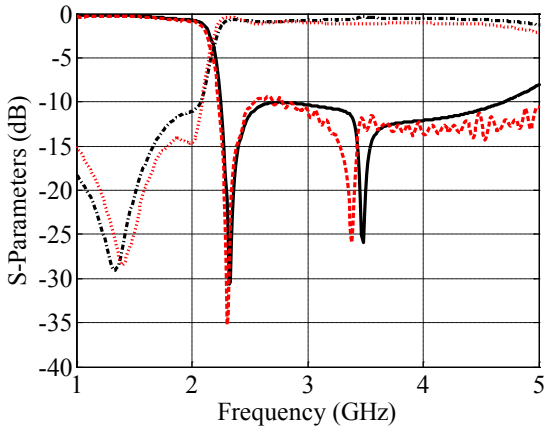

Fig. 8b. Same as Fig. 8a except for a larger A_1 ring (a_1 is increased from 10 to 11.5 mm)

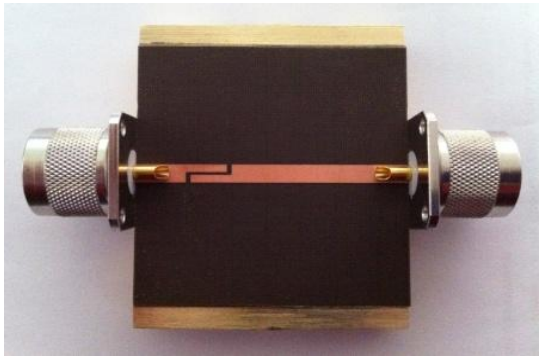

Fig. 9a. Photographs of the top side of fabricated bandpass filter.

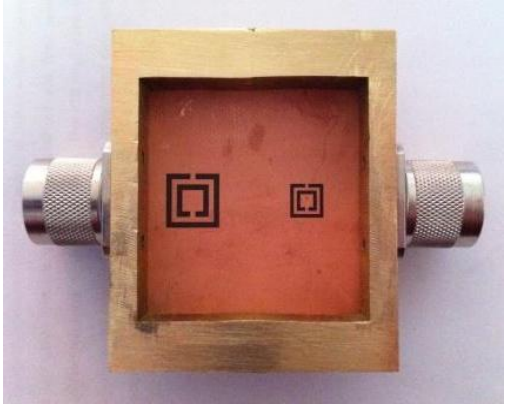

Fig. 9b. Photographs of the bottom side of fabricated bandpass filter.

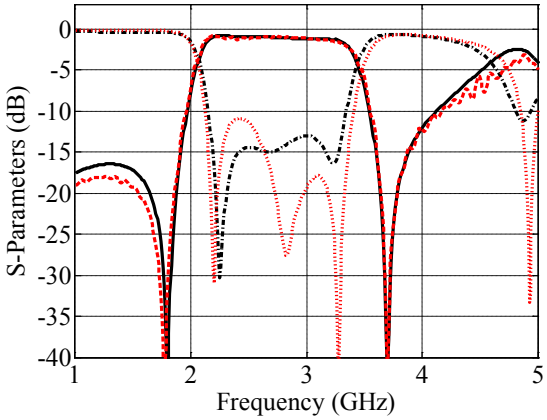

Fig. 10a. Simulation results compared to measured results of the proposed bandpass filters of Fig. 5. Simulated S_{21} and S_{11} are shown as (solid), (dash-dot) lines, respectively. Measured S_{21} and S_{11} are shown as (dashed) and (dotted) lines, respectively.

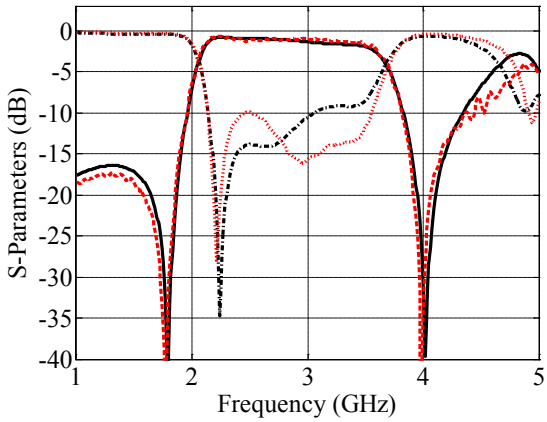

Fig. 10b. Same as Fig. 10a except for a larger (B2) ring.

REFERENCES

[1] V. Radisic, Y. Qian, R. Coccioli, and T. Itoh, "Novel 2-D Photonic Bandgap Structure for Microstrip Lines," *IEEE Microwave Guide Wave Lett.*, vol. 8, pp. 69 – 71, 1998.

[2] F. R. Yang, K. P. Ma, Y. Qian, and T. Itoh, "A Uniplanar Compact Photonic-Bandgap (UC-PBG) Structure and Its Applications for Microwave Circuits," *IEEE Trans. Microw. Theory Tech.*, vol. 47, no. 8, pp. 1509 – 1514, 1999.

[3] Y. Yang, Qian, R. Coccioli, and T. Itoh, "A Novel Low Loss Slow-Wave Microstrip Structure," *IEEE IEEE Microwave Guide Wave Lett.*, vol. 47, no. 8, pp. 372 – 374, 1998.

[4] J. S. Lim, C.-S. Kim, D. Ahn, Y.-C. Jeong, and S. Nam, "Design of Low-Pass Filters using Defected Ground Structure," *IEEE Transactions On Microwave Theory And Tech.*, vol. 53, no. 8, pp. 2539 – 2545, 2005.

[5] D. Ahn, J.-S. Park, C.-S. Kim, J. Kim, Y. Qian, and T. Itoh, "A Design of the Low-Pass Filter using the Novel Microstrip Defected Ground Structure," *IEEE Transactions On Microwave Theory And Tech.*, vol. 49, no. 1, pp. 86 – 93, 2001.

[6] M. K. Mandal and S. Sanyal, "A Novel Defected Ground Structure for Planar Circuits," *IEEE Microwave Compon. Lett.*, vol. 16, no. 1, pp. 93 – 95, 2006.

[7] H. Liu, Z. Li, and X. Sun, "Compact Defected Ground Structure in Microstrip Technology," *Electron. Lett.*, vol. 41, no. 3, pp. 132 – 134, 2005.

[8] B. Wu, B. Li, T. Su, and C.-H. Liang, "Study on Transmission Characteristic of Split-Ring Resonator Defected Ground Structure," *Progress In Electromagnetics Research*, vol. 2, no. 6, pp. 710 – 714, 2006.

[9] Z. –Z. Hou, X. –X. Li, and C. –K. Hao, "Design of Wideband Filter Using Split-ring Resonator DGS," *Progress In Electromagnetics Research Symposium, Hangzhou, China*, pp. 33-36, 2008.

[10] C Li and F. Li, "Characterization and Modelling of a Microstrip Line Loaded with Complementary Split-Ring Resonators (CSRRs) and its Application to Highpass Filters," *Journal of Physics D: Applied Physics*, vol. 40, pp. 3780 – 3787, 2007.

[11] J. B. Pendry, A. J. Holden, D. J. Robbins, and W. J. Stewart, "Magnetism from Conductors and Enhanced Nonlinear Phenomena," *IEEE Transactions on Microwave Theory and Tech.*, vol. 47, no. 11, pp. 2075 – 2084, 1999.

[12] F. Falcone, T. Lopetegi, M. A. G. Laso, J. D. Baena, J. Bonache, M. Beruete, R. Marque´s, F. Martı´n, and M. Sorolla, "Babinet Principle Applied to the Design of Metasurfaces and Metamaterials," *Physical Review Letters*, vol. 93, no. 19, pp. 197401-1 – 197401-4, 2004.

[13] M. Beruete, M. Sorolla, R. Marques, J. D. Baena, and M. Freire, "Resonance and Cross-Polarization Effects in Conventional and Complementary Split Ring Resonator Periodic Screens," *Electromagnetics*, vol. 26, Iss. 3 and 4, pp. 247-260, 2006.

[14] N. Ortiz, J. D. Baena, M. Beruete, F. Falcone, M. A. G. Laso, T. Lopetegi, R. Marque´s, F. Martin, J. Garcia-Garcia, and M. Sorolla, "Complementary Split-Ring Resonator for Compact Waveguide Filter Desing," *Journal of Microwaves, Optoelectronics and Electromagnetic Applications*, vol. 46, no. 1, pp. 88 – 92, 2005.

[15] L. H. Weng, Y. C. Guo, X. W. Shi, and X. Q. Chen, "An Overview on Defected Ground Structure," *IEEE Progress In Electromagnetics Research B*, vol. 7, pp.173 – 189, 2008.

[16] H.-W. Liu, Z.-F. Li, X.-W. Sun, S. Kurachi, J. Chen, and T. Yoshimasu, "Theoretical Analysis of Dispersion Characteristics of Microstrip Lines with Defected Ground Structure," *J. of Active and Passive Electronic Devices*, vol. 2, pp. 315 – 322, 2007.

[17] S. K. Parui and S. Das, "Improvement of Passband Characteristics of Microstrip Band Pass Filter by Defected Ground Structures," *The National Conference on Communications*, pp. 341 – 344, 2007.

[18] A. Boutejdar, A. Elsherbini, and A. Omar, "Design of a Novel Ultra-Wide Stopband Lowpass Filter using H-Defected Ground Structure," *Journal of Microwaves, Optoelectronics and Electromagnetic Applications*, vol. 50, no. 3, pp. 771 – 775, 2008.

[19] M. Al Sharkawy, A. Boutejdar, F. Alhefnawi, and O. Luxor, "Improvement of Compactness of Lowpass/Bandpass Filter Using a New Electromagnetic Coupled Crescent Defected Ground Structure Resonators," *Applied Computational Electromagnetic Society (ACES) Journal*, vol. 25, no. 7, pp. 570–577, July 2010.

[20] N. M. Garmjani and N. Komjani, "Improved Microstrip Folded Tri-Section Stepped Impedance Resonator Bandpass Filter using Defected Ground Structure," *Applied Computational Electromagnetic Society (ACES) Journal*, vol. 25, no. 11, pp. 975–983, November 2010.

[21] J. Zhang, B. Cui, S. Lin, and X.-W. Sun, "Sharp-Rejection Low-Pass Filter with Controllable Transmission Zero using Complementary Split Ring Resonators (CSRRs)," *Progress In Electromagnetics Research*, PIER 69, pp. 219 – 226, 2007.

[22] S. N. Khan, X. G. Liu, L. X. Shao, and Y. Wang, "Complementary Split Ring Resonators of Large Stop Bandwidth," *Progress In Electromagnetics Research Letters*, vol. 14, pp. 127 – 132, 2010.

[23] X. Lai, Q. Li, P. Y. Qin, B. Wu, and C.-H. Liang, "A Novel Wideband Bandpass Filter Based on Complementary Split-Ring Resonator," *Progress In Electromagnetics Research C*, vol. 1, pp. 177 – 184, 2008.

[24] S. K. Parui and S. Das, "Modeling of Split-Ring Type Defected Ground Structure and its Filtering Applications," *Journal of Microwaves, Optoelectronics and Electromagnetic Applications*, vol. 8, no. 1, pp. 6 – 12, 2009.